2002 HST Calibration Workshop
Space Telescope Science Institute, 2002
S. Arribas, A. Koekemoer, and B. Whitmore, eds.

STIS Calibration Status

Charles R. Proffitt[1,2], Paul Goudfrooij, Thomas M. Brown, James Davies, Rosa Diaz-Miller, Linda Dressel, Jessica Kim Quijano, Jesús Maíz-Apellániz, Bahram Mobasher, Mike Potter, Kailash Sahu, David Stys, Jeff Valenti, Nolan Walborn, Ralph Bohlin, Paul Barrett, Ivo Busko, and Phil Hodge

Space Telescope Science Institute, Baltimore, MD 21218

Abstract. Last year's failure of the STIS Side-1 electronics temporarily suspended use of the instrument. The Side-1 electronics are not repairable, but operations were resumed in August of 2001 using the redundant Side-2 electronics. STIS was fully returned to operation, with only minimal impacts on scientific performance.

MAMA detector performance continues to be very good, with sensitivity changes of 1 to 2 percent per year. Although the detailed relation between the NUV MAMA detector temperature and dark current has changed, typical NUV dark current levels are similar to those in previous cycles. The FUV dark current varies irregularly, and it is now usually significantly higher than it had been during the first two years of STIS operations.

The effects of radiation damage on the STIS CCD detector continue to follow previous trends, with declining charge transfer efficiency, increasing dark current, and increasing numbers of hot pixels. We also review the use and calibration of the E1 aperture positions which can be used to ameliorate CTE effects.

1. Side 1 Electronics Failure

A fuse on the main STIS power bus blew on May 16, 2001, safing the STIS instrument. A diagnostic test that was intended to repower the primary Side-1 electronics in stages by using an alternate power bus, resulted in another blown fuse as soon as the first STIS internal relay was closed. After review of the available telemetry and detailed engineering analyses, the failure review board (Davis et al. 2001) identified a number of possible causes, but concluded that the most likely cause was a shorted tantalum capacitor. There is essentially no chance that this type of capacitor could be melted open once shorted, and on-orbit repair appears to be impractically complex. It was concluded that no portion of the Side-1 electronics can be recovered.

Fortunately, STIS has a redundant set of electronics (Side-2), which was successfully used to reactivate STIS in early July 2001. The MAMA detectors and most instrument mechanisms perform much as they did on Side 1. However, because the Side-2 electronics lack a functioning temperature sensor for the STIS CCD detector, the CCD can no longer be operated at constant temperature. Instead, the thermo-electric cooler is operated at constant current, and while the mean detector temperature is actually lower than the -83 C Side-1 set point, both the CCD temperature and dark current vary significantly (Brown 2001a). The STIS CCD also suffers from a $\approx$1 e^-/pixel increase in read noise due to electronic pickup from the Side-2 electronics. This noise can under some circumstances be

[1]Science Programs, Computer Sciences Corporation

[2]Catholic University of America Institute for Astrophysics and Computational Science

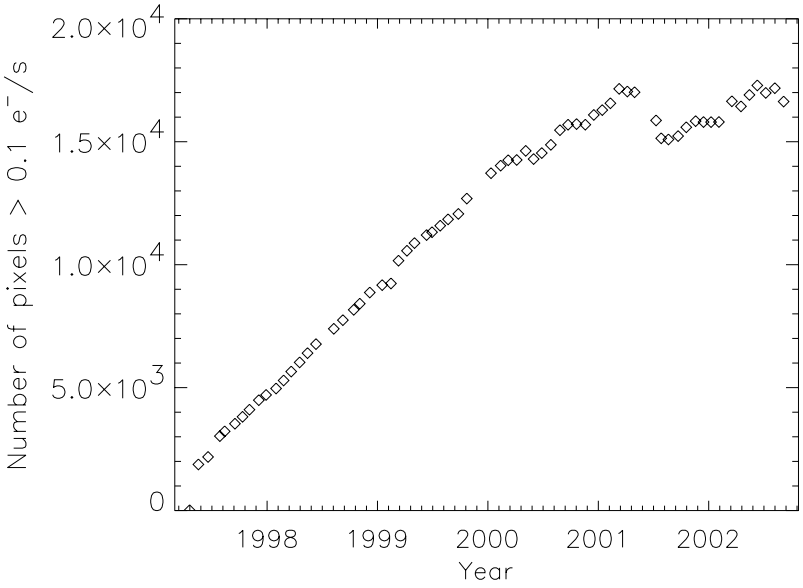

Figure 1. The number of CCD hot pixels vs. time. The apparent drop in mid-2001 is caused by the lower mean operating temperature of the CCD under Side-2 operations. Because the brightness of a given hot pixel decreases with decreasing detector temperature, at a lower temperature fewer pixels exceed a given fixed threshold.

ameliorated by Fourier filtering of the image (Brown 2001b). These differences are also discussed by Brown (2003) in these proceedings.

2. Detector Performance

Other than the differences between Side-1 and Side-2 discussed above, changes in STIS CCD detector performance continue previous trends—apart from some scaling differences caused by the lower mean CCD detector temperature under Side-2 operations. The number of hot pixels (Figure 1) and the typical dark current continues to increase as radiation damage accumulates on the detectors. As of September 2002, the mean STIS CCD dark rate is 0.026 e^-/pixel/s, and, after eliminating hot pixels, the median dark rate is 0.004 e^-/pixel/s. The charge transfer efficiency (CTE) continues to degrade, and is discussed in detail by Goudfrooij et al. (2003).

The MAMA detectors were not directly affected by the switch to the Side-2 electronics; however, there are some long term changes in the behavior of the detectors that can affect the calibration. Changes in the detector sensitivity over time are discussed in these proceedings by Bohlin (2003) and by Stys (2003). Here we will review long term changes in the behavior of the MAMA dark currents.

NUV MAMA Dark Current. The NUV MAMA dark current is dominated by phosphorescence of impurities in the MgF_2 faceplate of the detector. These impurities contain metastable states which become populated by charged particle impacts, especially during SAA passages, which can decay several days later, emitting UV photons. A model of the dark current was developed by Jenkins (1997, private communication) and Kimble (1997) (see also Ferguson & Baum 1999), and predicts that over short time scales the dark current will vary exponentially with temperature. Over longer time scales the behavior will depend

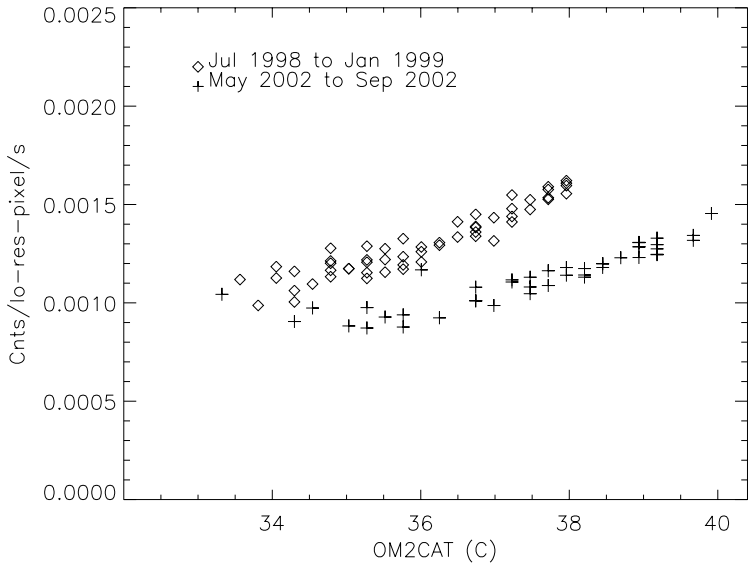

Figure 2. The NUV MAMA dark current versus detector temperature for two different time periods.

on the detailed temperature history of the detector window as well as on any variation in the number of charged particle impacts. The model predicts that long term increases in detector temperature will also lead to an increase in the mean NUV dark current, although with a slope much shallower than the short time scale variations with temperature.

Prior to SM3a in early 2000, both the mean detector temperature and the mean dark current were increasing over time. However, since that time, the average NUV MAMA dark current has been *decreasing*, even though detector temperatures have continued to increase. During Cycle 11, the mean NUV dark current has been about 12% lower than during Cycle 8 (Figure 2). Also note that even when detector temperatures are very low, the dark rate no longer drops below about 0.0009 cnts/s/lo-res-pixel. The scaling formula used in the STIS pipeline has been updated for these changes in behavior. New NUV dark reference files are also periodically delivered to account for small changes in the distribution of dark current across the detector.

FUV MAMA Dark Current. The FUV MAMA does not suffer from the phosphorescent glow seen in the NUV MAMA, and as a result it has a much lower dark current than other STIS detectors. It does, however, suffer from an intermittent glow of unknown origin centered in the upper left quadrant of the detector (Figure 3). This glow has become patchier and more frequent over time. The lower right corner remains free of the glow, with a mean dark rate of 6.6×10^{-6} cnts/s/pixel.

The average FUV MAMA dark rate has been increasing over time, and, at any given time, tends to increase with increasing detector temperature (Figure 4). However, the strongest correlation appears to be with the length of time that the MAMA high voltage has been turned on. Typically the MAMA high voltages are turned off prior to the block of *HST* orbits that pass through the South Atlantic Anomaly (SAA), and are turned back on after this block of orbits. The result of these policies is that FUV MAMA observations taken on the very first orbit after the high voltage has been turned back on will usually have very low dark currents, with little contribution from the intermittent glow. However, as there is only one such orbit available per day, it is not practical to reserve that orbit for

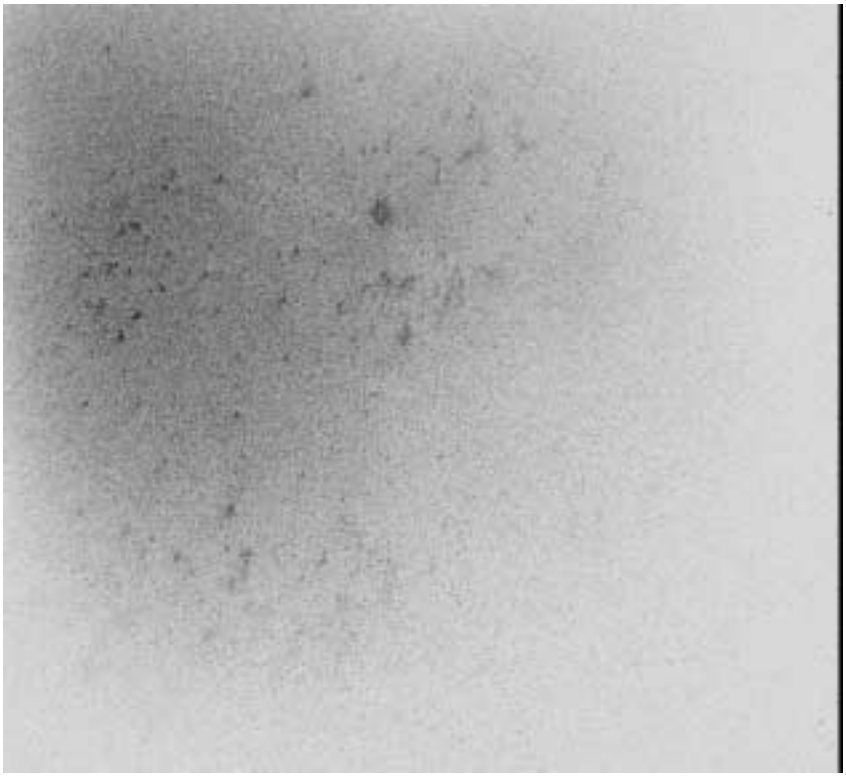

Figure 3. FUV MAMA dark current. This figure is the mean of dark monitor exposures taken between July 2001 and September 2002. Dark regions in this figure correspond to areas of higher dark current.

FUV programs that would benefit from a very low dark current, as doing so would have too large an impact on the flexibility needed for efficient scheduling of *HST*.

We instead recommend that very faint targets be placed in the darkest part of the detector. For very faint point source spectra, putting the spectrum about $2''$ above the bottom edge of the detector (POS TARG 0 -6.8), will put the spectrum in a region of much lower dark current (see Figure 5). We plan to introduce and calibrate a new pseudo-aperture position for this purpose during Cycle 12.

External cooling of the FUV MAMA detector would likely result in some decrease in the typical dark current, but it probably will not completely restore the very low dark currents that were commonly seen during the first two years of operation.

The number of hot pixels in the FUV MAMA has also been increasing with time. The number of hot pixels tends to correlate well with the mean intensity of the glow. New dark reference files have recently been delivered to track this increase.

3. E1 Aperture Positions for Reducing CTE Effects

The decline in CCD charge transfer efficiency (CTE), as radiation damage has accumulated on the detector, causes declines in the measured signal that depend both on the detected signal level as well as on the location of the image or spectrum on the detector (see Goudfrooij 2003 elsewhere in these proceedings). Starting in Cycle 9, new "pseudo-aperture" positions were defined for 1st order spectroscopy that allow targets to be easily placed near the top of the CCD. This reduces the number of parallel charge transfers from ≈ 512 to ≈ 124, and proportionately reduces the electrons lost to charge traps during the readout.

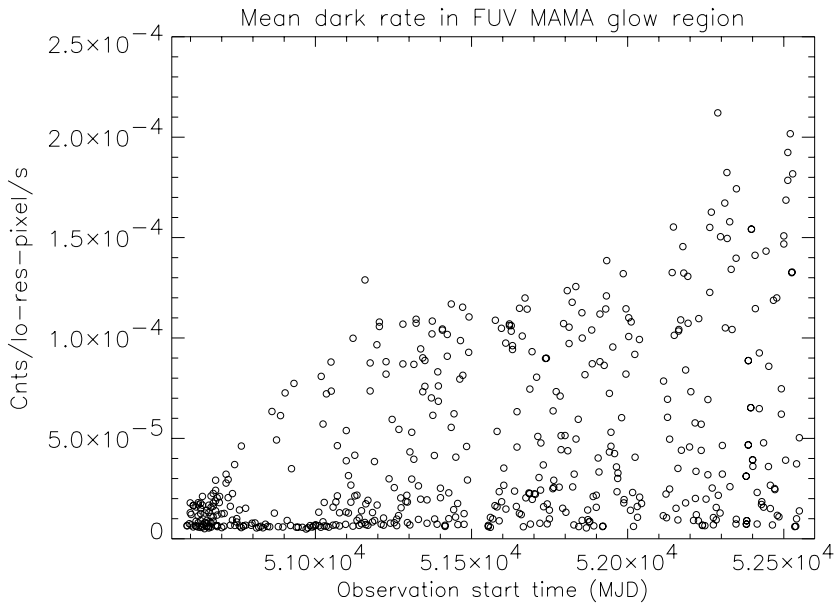

Figure 4. FUV MAMA dark current in glow region vs. time.

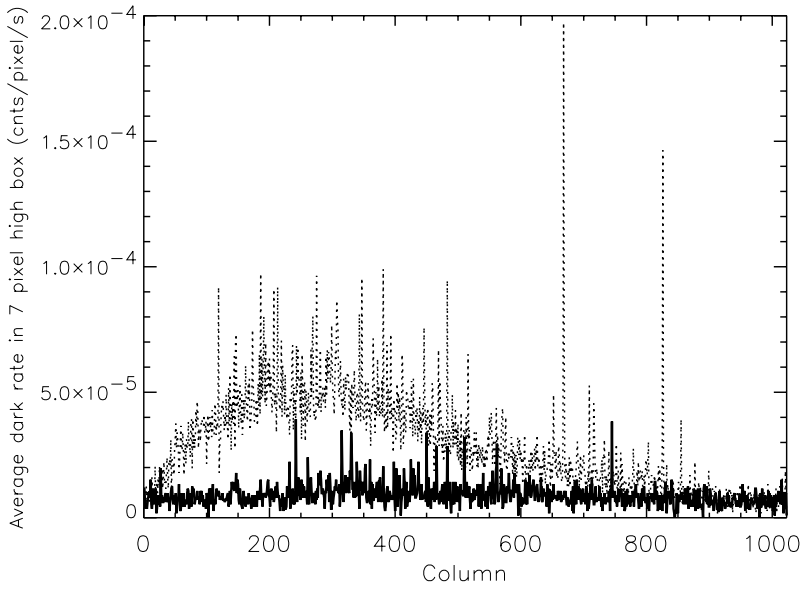

Figure 5. The FUV MAMA mean dark current vs. detector column, in a seven pixel high extraction box near the standard extraction position ($-3''$ below the detector center, dotted line) and in a box near the proposed pseudo-aperture position ($6.8''$ further down, solid line) are compared. The data used are an average of 116 1380 second dark monitor exposures taken between July 2001 and September 2002. This illustrates the typical reduction in the dark current that will result from putting 1st order spectra $2''$ above the bottom of the detector.

There are several advantages to using these new positions.

- Losing fewer electrons during the read-out directly increases the S/N.
- Because fractional CTE losses are larger at lower signal levels, the differential CTE losses can distort spectra. This can, for instance, change the apparent equivalent width of line features.
- Trapped electrons often reappear later during the read, causing "tails" to appear below bright features. This not only distorts the spatial profiles of real features, but these CTE tails below cosmic rays and hot pixels can be a serious source of noise for background or dark current limited observations. Putting the spectrum near row 900 dramatically reduces this kind of noise.

There are however, a few disadvantages to using the new E1 positions.

- The E1 aperture positions are only about 6″ below the top of the detector and about 6″ above the upper aperture bar; there is therefore less room for extended objects.
- For point source spectra at $\lambda > 7500$ Å, the use of contemporaneous IR flats for removing fringes (Goudfrooij & Christensen 1998) does not work as well as it does near the center of the detector. If S/N > 50 : 1 is needed at long wavelengths, we recommend using the regular aperture positions near row 512. For data taken at the E1 position, consideration should also be given to the use of Malumuth's (2003) procedure for constructing fringe flats.
- Some calibrations are not yet as well established near the E1 position as they are for data taken near the center of the detector. Extensive observations to improve the calibration of the sensitivity, dispersion, line-spread-functions, point-spread-functions, and aperture throughputs near the E1 positions have been collected during Cycles 10 and 11. We anticipate that the quality of the calibration at the E1 aperture positions during Cycle 12 will be nearly as high as it is for spectra taken near the center of the detector.

4. Recent and Pending Calibration Enhancements

A number of recent improvements have been made to the STIS pipeline calibration. A number of these are detailed in the paper by Diaz-Miller et al. (2003), and in other papers in these proceedings. Below we will discuss the most significant of these recent changes, as well as the improvements we plan to deliver in the near future.

Sensitivity Changes over Time. There have been clear changes in the sensitivity of the MAMA detectors over time. These changes vary with wavelength and detector, with sensitivity declining as much as 3% per year at the long wavelength end of the G140L wavelength range. NUV MAMA modes appear to have increased in sensitivity for the first year of STIS operations, but have since begun to decrease in sensitivity by 1 to 2% per year (Bohlin 1999; Stys & Walborn 2001; Stys et al. 2003). The STIS calibration pipeline now corrects 1st order MAMA spectroscopic modes for these changes in time dependent sensitivity. MAMA imaging modes also appear to show similar time and wavelength dependent sensitivity changes. The **synphot** package in the Space Telescope Data Analysis System (STSDAS) is currently being updated to allow the proper MAMA sensitivity curves to be used for any specified date. Evaluation of MAMA echelle modes is still in progress and we hope to include time dependent sensitivity corrections for these modes in the near future.

Measurements of the time dependent changes in CCD sensitivity are complicated by the degradation of CCD charge transfer efficiency (CTE). Losses due to CTE effects depend

on the signal level, the background level, and the position on the detector and need to be handled separately from time and wavelength dependent throughput changes. Both effects are currently being calibrated (see Goudfrooij 2003, and Bohlin 2003 in these proceedings), and we hope, in the near future, to also include time dependent sensitivity corrections for CCD modes in both the standard pipeline calibration and **synphot**.

Other recent improvements affecting flux calibration include delivery of a low order flat for G140L observations that corrects for vignetting effects at different target positions along the detector y axis (i.e., perpendicular to the dispersion direction). Similar flats for CCD 1st order modes are in preparation. Improved pixel-to-pixel flats are also being generated for both MAMA and CCD modes and will improve the calibration for very high signal-to-noise observations.

Improvements to Echelle Calibration. Among recent enhancements to the calibration of echelle data, the adoption in the pipeline of an improved algorithm for the subtraction of scattered light (Valenti et al. 2002, 2003) is especially noteworthy.

Also important is the pipeline implementation of a fix for flux calibration problems caused by shifts in the blaze function. This problem and its solution are described in detail by Bowers & Lindler (2003) elsewhere in these proceedings. The largest part of the problem resulted from the monthly offsetting of the location of the spectrum on the detector, and while this offsetting was turned off for echelle spectral modes starting in August 2002, it is still necessary to correct earlier spectra affected by this problem. Currently the pipeline uses Bowers & Lindler's algorithm to correct data taken at the primary echelle wavelength settings. New dispersion relations which better account for the effects of the monthly offsetting on the echelle wavelength solution have also been delivered to the pipeline.

Other Enhancements Under Development. A number of other improvements in both pipeline software and post-pipeline analysis tools are currently under development. Below are some of the items we hope to complete and make available to the STIS user community in the near future.

- CTE correction formulae for both imaging and spectroscopic observations (see Goudfrooij et al. 2003).
- Better NUV-PRISM flux and wavelength calibrations for both on-axis and off-axis observations.
- Improved software tools for the analysis of slitless spectra, that will allow quick matching of objects observed in both dispersed and undispersed light and easier extraction of properly calibrated 1-D spectra.
- More and better options for background smoothing or interpolation for 1st order spectroscopic modes.
- Increased on-line selection of imaging and spectroscopic PSFs for post-pipeline analysis.
- Time dependent sensitivity corrections for all modes.
- More accurate flux calibration for all secondary wavelength settings, including echelle blaze shift effects.

References

Bohlin, R. C. 1999, *Changes in Sensitivity of the Low Dispersion Modes*, *Instrument Science Report* STIS 99-07, (Baltimore: STScI)

Bohlin, R. C. 2003, this volume, 115

Bowers, C. & Lindler, D. 2003, this volume, 127

Brown, T. M. 2001a, *Temperature Dependence of the STIS CCD Dark Rate During Side-2 Operations*, *Instrument Science Report* STIS 2001-003 (Baltimore: STScI)

Brown, T. M. 2001b, *STIS CCD Read Noise During Side-2 Operations*, *Instrument Science Report* STIS 2001-005 (Baltimore: STScI)

Brown, T. M. 2003, this volume, 180

Davis, M., Campbell, D., Sticka, R., Faful, B., Leidecker, H., Kimble, R., & Goudfrooij, P. 2001, *STIS Failure Review Board Final Report* (Baltimore: STScI)

Diaz-Miller et al. 2003, this volume, 189

Ferguson, H. & Baum, S. 1999, *Scientific Requirements for Thermal Control and Scheduling of the STIS MAMA Detectors after SM-3*, *Instrument Science Report* STIS 99-02 (Baltimore: STScI)

Goudfrooij, P. 2003, this volume, 105

Goodfrooij, P. & Christensen, J. A. 1998, *STIS Near-IR Fringing. III. A Tutorial on the Use of the IRAF Tasks*, *Instrument Science Report* STIS 98-29 (Baltimore: STScI)

Kimble, R. 1997, STIS IDT Quicklook Analysis Report no. 37, *Temperature/Time Modeling of MAMA2 Phosphorescent Dark Rate*

Malumuth, E. 2003, this volume, 197

Stys, D. J. & Walborn, N. R. 2001, *Sensitivity Monitor Report for the STIS First-Order Modes-III*, *Instrument Science Report* STIS 2001-01R (Baltimore: STScI)

Stys, D., et al. 2003, this volume, 205

Valenti, J. A., Lindler, D., Bowers, C., Busko, I., Kim Quijano, J. 2002, *'2-D Algorithm for Removing Scattered Light from STIS Echelle Data*, *Instrument Science Report* STIS 2002-001 (Baltimore: STScI)

Valenti, et al. 2003, this volume, 209